Journal of the Korean Magnetic Resonance Society **2005**, *9*, 93 - 102

Development of 3D Mapping Algorithm with Non Linear Curve Fitting Method in Dynamic Contrast Enhanced MRI

Seong-Ik Yoon[1], Geon-Ho Jahng[2], Hyun-Soo Khang[3], Young-Joo Kim[4] and Bo-Young Choe[1*]

[1]Department of Biomedical Engineering, College of Medicine, The Catholic University of Korea, [2]Department of Radiology, University of California at San Francisco, [3]Department of Radiology, Seoul Health College, [4]Department of Radiology, College of Medicine, The Catholic University of Korea

Received August 4, 2005

Abstract : Purpose : To develop an advanced non-linear curve fitting (NLCF) algorithm for dynamic susceptibility contrast study of brain.

Materials and Methods: The first pass effects give rise to spuriously high estimates of K^{trans} in voxels with large vascular components. An explicit threshold value has been used to reject voxels.

Results: By using this non-linear curve fitting algorithm, the blood perfusion and the volume estimation were accurately evaluated in T2*-weighted dynamic contrast enhanced (DCE)-MR images. From the recalculated each parameters, perfusion weighted image were outlined by using modified non-linear curve fitting algorithm. This results were improved estimation of T2*-weighted dynamic series.

Conclusion: The present study demonstrated an improvement of an estimation of kinetic parameters from dynamic contrast-enhanced (DCE) T2*-weighted magnetic resonance imaging data, using contrast agents. The advanced kinetic models include the relation of volume transfer constant K^{trans} (min^{-1}) and the volume of extravascular extracellular space (EES) per unit volume of tissue υ_e .

Keywords: NLCF, dynamic contrast-enhanced (DCE), kinetic parameters

INTRODUCTION

The advantage of magnetic resonance imaging (MRI) based on perfusion imaging method is that, in addition to its noninvasiveness, the option of using other nuclear magnetic

* To whom correspondence should be addressed. E-mail : bychoe@catholic.ac.kr

resonance techniques (e.g., diffusion-weighted imaging, metabolite spectroscopy, tissue relaxometry) is available.[1,2] The dephasing of randomly perfusing water protons (intravoxel incoherent motion) in magnetic field gradients as an index of tissue perfusion, was thwarted by the inadequacy of the hardware available to provide sufficient image dynamic range for useful quantification of perfusion.[3] Attempts to produce quantified images of blood volume and endotherial permeability from dynamic or MRI data were reported.[4,5]

The dynamic enhancement data have been modeled by repeated T1-weighted imaging of tissue after injection of Gd-DTPA.[6] Most of the signals in a ROI or Pixel consist of information about blood flow, capillary leakage, and related physiological parameters.[7-10] The improved temporal resolution of dynamic MRI sequences requires the short-lived variations in signal intensity which occurs during the first passage of a bolus of contrast agent.[11]

On the other hands, arterial spin labeling (ASL) uses radiofrequency (RF) pulses to magnetically label moving spins in flowing blood.[12,13] The issue of accuracy and reproducibility of calculated pharmacokinetic parameters such as perfusion, blood volume etc was reported.[14-16] The MR contrast agents with cerebral perfusion provide information about different physiologic parameters related to cerebral blood flow (CBF), cerebral blood volume (CBV) and mean transit time (MTT) of blood through a volume of tissue. To access the true physiological parameters, we approached new algorithm with non-linear curve fitting (NLCF) method for dynamic susceptibility contrast (DSC) study of brain.

The purpose of this study was to develop non-linear curve fitting algorithm for DSC study of brain. By using this non-linear curve fitting algorithm, the blood perfusion and the volume estimation were accurately evaluated in $T2^*$ weighted dynamic contrast enhanced (DCE)-MR images.

MATERIALS AND METHOD

Subjects and MR methods

Twenty healthy volunteers participated for the acquisition of T1-weighted and $T2^*$-weighted DCE MR imaging. Fifty single-shot echo-planar images were obtained in each of

19 slices in 74 seconds. As a imaging parameters, TR/TE were 1400/30, FOV of 23 x 23 cm image matrix of 128 x 128 pixels, section thickness of 5 ㎜ with a mini gap.

Standardized Quantities and Working Parameters

Most methods of analyzing DCE T1-weighted data have used a compartmental analysis to obtain some combination of the three principle parameters (1): k_{ep}, K^{trans}, v_e. The transfer constant and the extravascular extracellular space (EES) relate to the fundamental physiology, whereas the rate constant is the ratio of the transfer constant to the EES:

$$k_{ep} = K^{trans}/v_e. \text{ ----- (1)}$$

k_{ep}; The rate constant
K^{trans}; The transfer constant
v_e; fractional volume

The rate constant can be derived from the shape of the tracer concentration versus time data, whereas the transfer constant and EES require access to absolute values of tracer concentration. The transfer constant K^{trans} has several physiologic interpretations, depending on the balance between capillary permeability and blood flow in the tissue of interest. In high-permeability situations (where flux across the endothelium is flow limited), the transfer constant is equal to the blood plasma flow per unit volume of tissue:

$$K^{trans} = F\rho\ (1 - \text{Hct})\ (PS \gg F) \text{ ----- (2)}$$

F; Perfusion of whole blood per unit mass
ρ; Density of tissue
Hct; Hematocrit
PS; Permeability surface area product per unit mass of tissue

In the other limiting case of low permeability, where tracer flux is permeability limited, the transfer constant is equal to the permeability surface area product between blood plasma and the EES, per unit volume of tissue (2):

$$K^{trans} = PS\rho \ (PS \ll F) \text{ ----- (3)}$$

PS; Permeability surface area product per unit mass of tissue

New Modeling Feature

Flow-limited (Kety) model represented a model of flow-limited tracer uptake in tissue that has been used extensively. It was developed for the case of breathing an inert gas, which distributes into the whole tissue, including the intracellular spaces. In this model, differential equation relating tissue concentration C_t to arterial plasma concentration C_p is obtained in equation.

Permeability surface (PS) limited model indicated low permeability. If flow is high, the blood plasma can be considered as a single pool, with equal arterial and venous concentrations. The transport of tracer out of the vasculature is slow enough not to deplete the intravascular concentration. For accurate and ideal approach of NLF, it has been added Y value in the modified generalized kinetic model.

Flow-Limited (Kety) Model

$$dC_t/dt = F_\rho(1 - Hct)\ (C_p - C_t/v_e)$$

Generalized kinetic Model

$$dC_t/dt = K^{trans}(C_p - C_t/v_e) = K^{trans}\ C_p - K_{ep}\ C_t$$

Equation [1]

Modified Generalized Kinetic Model with NLF

$$dC_t/dt = K^{trans}(C_p - C_t/v_e) * Y = K^{trans}\ C_p - K_{ep}\ C_t$$

Y : Coefficient Factor

Equation. [2]

Clinical Imaging

The 1.5T Siemens Avanto Scanner was employed with the maximum gradient power 40 mT/m. Routine MRI was performed using T1W images and a sequential set obtained using GRE-EPI sequence. For viewing of whole brain, applied sequence has been increased slice numbers. Sequential images were continuously recorded during the first passage of contrast agent with the signal intensity for ROI. For the safe delivery of required gadolinium we used the automatic injection pump at standard rates.

Since the transit time of the bolus through the tissue is only a few seconds, high temporal resolution imaging is required to obtain sequential images during the wash in and wash out of the contrast material and resolve the first pass of the tracer. This procedure was essential for all volunteer to more advantageous steps to review the numerical values. Thus, generalized kinetic model with NLF was modified with the consideration of coefficient factor.

RESULTS

The relaxation rate of blood was changed by the injection of a contrast agent in the blood pool. This change was related to CBF, CBV and MTT of blood through a volume of tissue. The absorbed rates in tissue T2 (Fig.1A) and $T2^*$ following the injection of an MR contrast agent were mainly due to the dephasing of the extravascular spins in the spatially non-uniform field created by the magnetic susceptibility differences between vascular and extravascular compartments.

The absence of diffusion motion, R2 was depended on the size and the architecture of the vascular compartment. For increased doses of contrast agent, the curve $\Delta R2$ was drifted on the basis of the doses of contrast agents. Levenberg-Marquardt non-linear least square fitting algorithm was modified to accomplish the effective fitting of the pixels (Fig.1B).

Multicompartment models of contrast distribution are based on the assumption that contrast is evenly distributed throughout the blood volume before leakage into the extracellular space occurs.[22] For more precise combination of numerical integration of its $\Delta R2$ time curve and deconvolution between the arterial input and the $\Delta R2$ curve is perform-

ed. Arterial input function (AIF) was identified from the middle cerebral artery on the normal side (Fig.2). After then, recalculated each parameter, perfusion weighted image (PWI) were outlined by using modified NLF algorithm. This results were improved estimation of $T2^*$-weighted dynamic series.

DISCUSSION AND CONCLUSIONS

The ultimate goal of MRI perfusion studies is the assessment of regional perfusion from MR image intensity. One approach involves the use of endogenous or exogenous blood pool tracers, that is, tracers that stay within the intravascular space. The anteriolar, capillary, and venular volumes were reported to be approximately 21%, 33%, and 46% of the total microvascular blood volume.[4] The CBV may also be split into cerebral plasma volume (CPV) and cerebral red cell volume (CRCV). Non-NMR techniques to measure CPV and CRCV in humans and large animals include positron emission tomography (PET) and single photon emission tomography (SPECT).

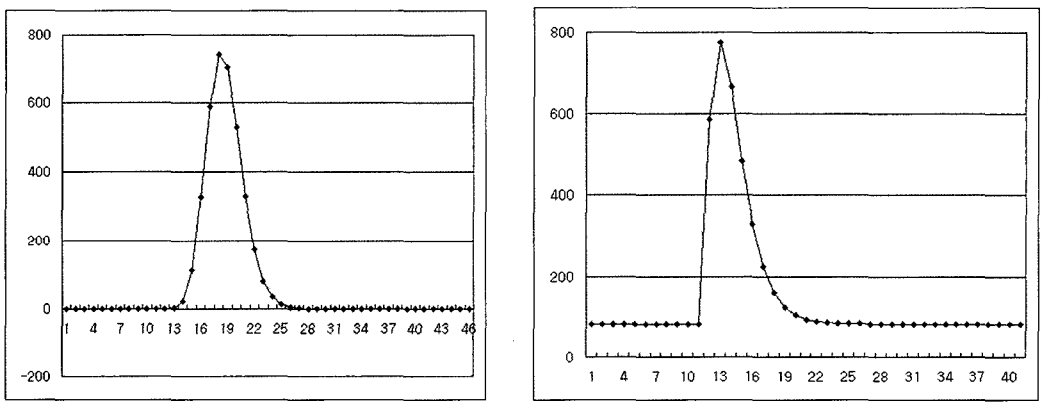

(A) (B)

Fig. 1. Curve fitting with New Algorithm, (A) Conventional signal conversion with ΔR2 (B)Gamma-variation curve fitting with Levenberg-Marquardt.

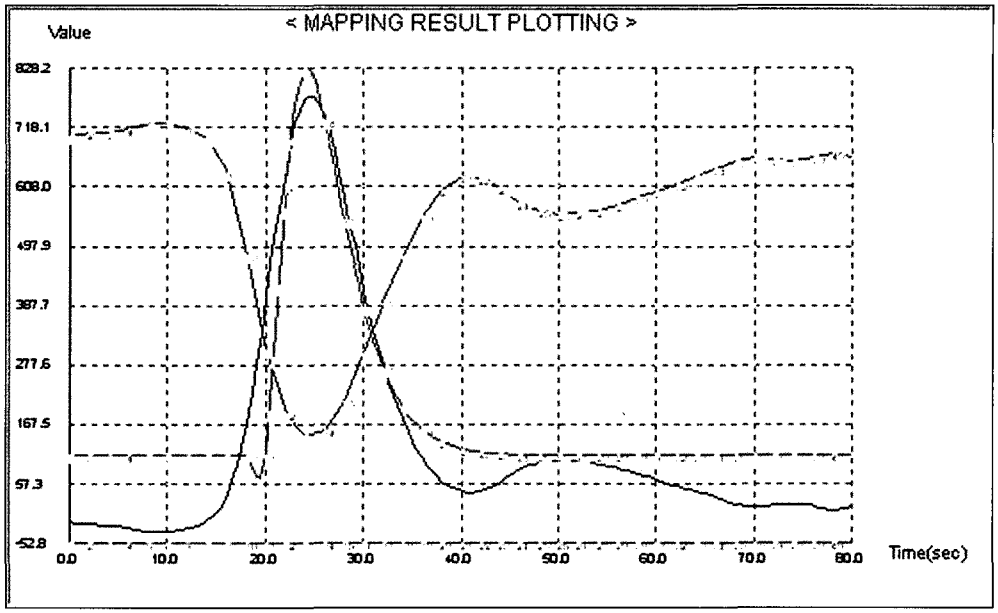

Fig. 2. Mapping result plotting of AIF.

T1-wighted DCE imaging has been used to measure relative blood volume based on transient T1 changes during the first pass of contrast bolus in patients with brain tumors.[2, 17, 18] However, T1-CBV(r) measurements overestimate blood volume where contrast leakage occurs. In comparison, $T2^*$-CBV(r) maps calculated from susceptibility contrast enhanced images can underestimate tumor blood volume due to residual T1 effects, known as T1 shine through, which compete with the $T2^*$ signal change in the presence of contrast leakage Several techniques have been suggested to reduce T1 shine-through, including imaging sequences with low T1 weighing pre-enhancement using small or large doses of contrast to saturate T1 effects.[20,21] After elimination of T1 shine-through, values on the $T2^*$-CBV(r) map may be considered as true reflections of tissue blood volume. The simultaneous mapping approach is attractive since the signal change due to contrast leakage, which causes the T1 shine-through, is removed from the contrast concentration time course and can be used to provide estimates of endothelial permeability. Although the mean rCBV, diffusion weighted (DW) image intensity, apparent diffusion coefficient (ADC), and fractional anisotropy (FA) ratios for hypoperfused tissue that progressed to infarction and hypoperfused tissue that remained viable have more overlap, they provide adjunctive information.

In conclusion, we developed non-linear curve fitting algorithm for DSC study. And the data point from the gamma-variation curve fitting with Levenberg-Marquardt could be useful to achieve the physiological information in the clinical cases.

Acknowledgment

This study was supported by a grant of the Korea Health 21 R&D Project, Ministry of Health & Welfare, Republic of Korea (02-PJ3-PG6-EV07-0002) and a grant of the 2005 Nuclear R&D Plan Program, Ministry of Science & Technology, Korea.

REFERENCES

1. Tofts PS, Brix G, Buckley DL, et al. Estimating kinetic parameters from dynamic contrast-enhanced T1-weighted MRI of a diffusible tracer: Standardized quantities and symbols. *JMRI*, 10, 223-232 (1999).
2. Li KL, Jackson A. New hybrid technique for accurate and reproducible quantitation of dynamic contrast-enhanced MRI data. *Magn Reson Med* , 50, 1286-1295 (2003).
3. Calamante F, Pell GS, Thomas DL. Measuring cerebral blood flow using magnetic resonance imaging techniques. *J Cereb Blood Flow Metab* , 19, 701-735 (1999).
4. Barbier EL, Lamalle L, Décorps M. Methodology of brain perfusion imaging *JMRI* , 13 496-520 (2001).
5. Xavier G, Jeroen H, Tchoyoson L. Perfusion Imaging Using Arterial Spin Labeling. *Topics in Magnetic Resonance Imaging*, 15, 10-27 (2004).
6. Howard RA, Timothy PL. Clinical Perspectives in Perfusion: Neuroradiologic Applications. *Topics in Magnetic Resonance Imaging*, 15, 28-40 (2004).
7. Jahng GH, Zhu XP, Matson GB, Weiner MW, Schuff N. Improved perfusion-weighted MRI by a novel double inversion with proximal labeling of both tagged and control acquisitions. *Magn Reson Med.*, 49, 307-314 (2003).

8. Li KL, Zhu XP, Hylton N, Jahng GH, Weiner MW, Schuff N. Four-phase single-capillary stepwise model for kinetics in arterial spin labeling MRI. *Magn Reson Med* ., 53 511-518 (2005).
9. Richard B. Buxton et al. A General Kinetic Model for Quantitative Perfusion Imaging with Arterial Spin Labeling. *Magn Reson Med.*, 40, 383-396 (1998).
10. Luh WM, Wong EC, Bandettini PA, Hyde JS. QUIPSS II with thin-slice TI_1 periodic saturation: A method for improving accuracy of quantitative perfusion imaging using pulsed arterial spin labeling. *Magn Reson Med* ., 41, 1246-1254 (1999).
11. Lai S, Wang JJ, Jahng GH. FAIR exempting separate T_1 measurement (FAIREST): a novel technique for online quantitative perfusion imaging and multi-contrast fMRI *NMR in Biomedicine*, 14, 507-516 (2001).
12. Wang JJ, Alsop DC, Li L., Listerud J, Gonzalez JB, Schnall MD, Detre JA. Comparison of quantitative perfusion imaging using arterial spin labeling at 1.5 and 4.0 Tesla. *Magn Reson Med* , 48, 242-254 (2002).
13. Johnson NA, Jahng GH, Weiner MW, et al. Pattern of Cerebral Hypoperfusion in Alzheimer Disease and Mild Cognitive Impairment Measured with Arterial Spin-labeling MR Imaging: *Initial Experience Radiology* , 234, 851-859 (2005).
14. Jahng GH, Song EM, Zhu XP et al. Human Brain: Reliability and Reproducibility of Pulsed Arterial Spin-labeling Perfusion. *MR Imaging* Radiology , 234, 909-916 (2005).
15. Kennan RP, Rolf Jäger HR. T_2- and T_2*-W DCE-MRI: Blood Perfusion and Volume Estimation using Bolus Tracking , Quantitative MRI of the Brain, 2003 John Wiley & Sons, Ltd
16. Daldrup H, Shames DM, Husseini W, et al. Quantification of the extraction fraction of gadopentetate across breast tumor capillaries. *Magn Reson Med.*, 40, 537–543 (1998).
17. Cha SM, Knopp EA, Johnson G, Andrew Litt A, Glass J, Gruber ML, Lu S, and Zagzag D. Dynamic Contrast-enhanced T2*-weighted MR Imaging of Recurrent Malignant Gliomas Treated with Thalidomide and Carboplatin *Am J Neuroradiol,* 21, 881-890 (2000).
18. Cha SM, Knopp EA, Johnson G, Wetzel SG, Andrew W. Litt, and David Zagzag. Intracranial Mass Lesions: Dynamic Contrast-enhanced Susceptibility-weighted Echo-planar Perfusion. *MR Imaging Radiology* , 223, 11-29 (2002)

19. Schaefer PW, Ozsunar Y, Julian HE, Leena M. Hamberg, Hunter GJ, Sorensen AJ, Koroshetz WJ, and Gonzalez RG. Assessing Tissue Viability with MR Diffusion and Perfusion Imaging. *Am. J. Neuroradiol., Mar.*, 24, 436-443 (2003).
20. Bruening R, Kwong KK, Vevea MJ, et al. Echo-planar MR determination of relative cerebral blood volume human brain tumors: T1 versus T2 weighting. *Am. J. Neuroradiol.*, 17, 831–840 (1996).
21. Hacklander T, Reichenbach JR, Hofer M, et al. Measurement of cerebral blood volume via the relaxing effect of low-dose gadopentetate dimeglumine during bolus transit. *Am. J. Neuroradiol.,* 17, 821–830 (1996).
22. Li KL, Zhu XP, Waterton J, Jackson A. Improved 3D quantitative mapping of blood volume and endothelial permeability in brain tumors. *J Magn Reson Imaging*, 12, 347–57 (2000).